2009 American Control Conference
Hyatt Regency Riverfront, St. Louis, MO, USA
June 10-12, 2009

Adaptive Robust Control: A Piecewise Lyapunov Function Approach

Jianming Lian, Jianghai Hu and Stanislaw H. Żak

Abstract— **The problem of output tracking control for a class of multi-input multi-output uncertain systems is considered. A novel adaptive robust controller is proposed, which incorporates a variable-structure radial basis function (RBF) network to approximate unknown system dynamics. The RBF network can determine its structure on-line dynamically, where radial basis functions are added or removed to ensure the desired tracking accuracy and to prevent the network redundancy simultaneously. The structure variation of the RBF network is taken into account in the stability analysis of the closed-loop system. This is accomplished by using the piecewise continuous quadratic Lyapunov function typically for the analysis of switched and hybrid systems.**

I. Introduction

In any controller design, one of the essential elements is a mathematical model of the plant to be controlled. However, the available mathematical model often contains uncertainties resulting from unknown system dynamics or disturbances. Recently, several adaptive controller design methodologies for uncertain systems have been introduced such as adaptive feedback linearization [1], adaptive backstepping [2], nonlinear damping and swapping [3] and switching adaptive control [4]. Especially, a number of adaptive control strategies have been developed for a class of feedback linearizable nonlinear systems including both single-input single-output (SISO) systems [5]–[8] and multi-input multi-output (MIMO) systems [9]–[12]. To improve the robustness of adaptive controllers, robustifying components have been used in [5], [7], [8], [10]–[12].

To deal with dynamical uncertainties, adaptive (robust) control strategies often involve certain types of function approximators to approximate unknown system dynamics. In particular, one-layer neural networks have been employed in [5], [11], where radial basis function (RBF) networks were used to approximate unknown system dynamics. However, fixed-structure RBF networks require the off-line determination of the appropriate network structure. In [6], [9], multilayer neural network (MLNN) based adaptive robust control strategies were proposed. Although it is not required to define the basis function sets for MLNNs, it is still necessary to pre-determine the number of hidden neurons. Moreover, compared with MLNNs, RBF networks are characterized by simpler structure, faster - computation time and superior adaptive performance. Variable structure RBF network based adaptive (robust) controllers have been proposed for SISO feedback linearizable uncertain systems in [8], [13], [14], where the variable-structure RBF networks that can both grow and shrink were employed. However, they are subject to the problem of infinitely fast switching between different structures. Moreover, the effect of the structure variation was not considered in the stability analysis.

In this paper, we consider, as in [9]–[12], the output tracking control problem for a class of MIMO feedback linearizable uncertain systems. We propose a novel adaptive robust control strategy. The developed controller incorporates a variable-structure RBF network, which is an improved version of the network considered in [14], [15], to approximate unknown system dynamics. The employed variable-structure RBF network avoids selecting basis functions off-line by determining the network structure on-line dynamically. It can add or remove RBFs depending on the magnitude of the output tracking error to ensure the tracking accuracy and to prevent the network redundancy simultaneously. We impose a dwelling time requirement on the structure variation to avoid the problem of infinitely fast switching between different structures as in [16]. The raised-cosine RBF (RCRBF) presented in [17] is utilized because the RCRBF has compact support that results in significant reduction of computations required for the network's training and output evaluation [15]. By viewing the closed-loop system as a switched system, we can apply the piecewise continuous quadratic Lyapunov function that has been used in the stability analysis of switched and hybrid systems [18], [19]. This enables us to analyze the structure variation in the stability analysis without additional restrictive assumptions.

The journal version of this paper with all the details and additional results can be found in [20].

II. System Description and Problem Statement

We consider a class of uncertain systems consisting of p coupled subsystems modeled by the following equations,

$$y_i^{(n_i)} = f_i(\boldsymbol{x}) + \sum_{j=1}^{p} g_{ij}(\boldsymbol{x})u_j + d_i, \quad i = 1, \ldots, p, \qquad (1)$$

where y_i, u_i and d_i are the output, input and disturbance of the i-th subsystem, respectively, and $f_i(\boldsymbol{x})$ and $g_{ij}(\boldsymbol{x})$ are unknown functions with

$$\boldsymbol{x} = \left[y_1 \ \cdots \ y_1^{(n_1-1)} \ \cdots \ y_p \ \cdots \ y_p^{(n_p-1)} \right]^\top$$

being the state vector of the overall system. The disturbance d_i can have the form of $d_i(t)$, $\boldsymbol{d}_i(\boldsymbol{x})$ or $\boldsymbol{d}_i(t, \boldsymbol{x})$. Let $(\boldsymbol{A}_i, \boldsymbol{b}_i)$ be the canonical controllable pair that represents a chain of n_i integrators, and let $\boldsymbol{c}_i = [1\ 0\ \cdots\ 0]_{1\times n_i}$, $\boldsymbol{y} = [y_1\ \cdots\ y_p]^\top$,

This work was supported by the Office of Naval Research Grant N00014-08-1-0080 and the National Science Foundation Grant CNS-0643805.

Jianming Lian, Jianghai Hu and Stanislaw H. Żak are with the School of Electrical and Computer Engineering, Purdue University, West Lafayette, IN 47907-2035, USA. {jlian,jianghai,zak}@purdue.edu.

$\boldsymbol{u} = [u_1 \ \cdots \ u_p]^\top$ and $\boldsymbol{d} = [d_1 \ \cdots \ d_p]^\top$. We represent the system (1) in a compact form as

$$\begin{aligned} \dot{\boldsymbol{x}} &= \boldsymbol{A}\boldsymbol{x} + \boldsymbol{B}\left(\boldsymbol{f}(\boldsymbol{x}) + \boldsymbol{G}(\boldsymbol{x})\boldsymbol{u} + \boldsymbol{d}\right) \\ \boldsymbol{y} &= \boldsymbol{C}\boldsymbol{x}, \end{aligned} \tag{2}$$

where $\boldsymbol{A} = \text{diag}[\boldsymbol{A}_1 \ \cdots \ \boldsymbol{A}_p]$, $\boldsymbol{B} = \text{diag}[\boldsymbol{b}_1 \ \cdots \ \boldsymbol{b}_p]$, $\boldsymbol{C} = \text{diag}[\boldsymbol{c}_1 \ \cdots \ \boldsymbol{c}_p]$, $\boldsymbol{f}(\boldsymbol{x}) = [f_1(\boldsymbol{x}) \ \cdots \ f_p(\boldsymbol{x})]^\top$ and $\boldsymbol{G}(\boldsymbol{x}) = [g_{ij}(\boldsymbol{x})]_{p\times p}$. The above system is often referred to as square system, because there are same numbers of inputs and outputs. As pointed out in [10], many physical systems, such as natural Lagrangian systems and circuit systems, can be modeled in the form of (1). In this paper, we assume that $\boldsymbol{f}(\boldsymbol{x})$ and $\boldsymbol{G}(\boldsymbol{x})$ are Lipschitz continuous vector- and matrix-valued functions of $\boldsymbol{x}$, respectively, $\boldsymbol{d}$ is Lipschitz continuous in $\boldsymbol{x}$ and piecewise continuous in t, and $\|\boldsymbol{d}\| \leq d_o$. In addition, we consider the case where the input matrix $\boldsymbol{G}(\boldsymbol{x})$ is definite with eigenvalues bounded away from zero for all $\boldsymbol{x}$ of interest. Without loss of generality, we assume that $\boldsymbol{G}(\boldsymbol{x})$ is positive definite with $\underline{g}\boldsymbol{I}_p \leq \boldsymbol{G}(\boldsymbol{x}) \leq \overline{g}\boldsymbol{I}_p$, where $\underline{g}$ and $\overline{g}$ are positive constants.

Our goal is to develop a tracking control strategy such that the i-th system output y_i, $i = 1, \ldots, p$, tracks a reference signal y_{di}. We assume that y_{di} has bounded derivatives up to the n_i-th order. Thus, we have $\boldsymbol{y}_d^{(n)} = [y_{d1}^{(n_1)} \ \cdots \ y_{dp}^{(n_p)}]^\top \in \boldsymbol{\Omega}_{y_d}$, where $\boldsymbol{\Omega}_{y_d}$ is a compact subset of $\mathbb{R}^p$. Then we define the desired system state vector as $\boldsymbol{x}_d = [y_{d1} \ \cdots \ y_{d1}^{(n_1-1)} \ \cdots \ y_{dp} \ \cdots \ y_{dp}^{(n_p-1)}]^\top$. We have $\boldsymbol{x}_d \in \boldsymbol{\Omega}_{x_d}$, where $\boldsymbol{\Omega}_{x_d}$ is a compact subset of $\mathbb{R}^n$. Let $e_i = y_i - y_{di}$ denote the i-th output tracking error. We define the output tracking error as $\boldsymbol{e}_y = [e_1 \ \cdots \ e_p]^\top$ and then the state tracking error as $\boldsymbol{e} = \boldsymbol{x} - \boldsymbol{x}_d$. It follows from (2) that the state tracking error dynamics are given by

$$\dot{\boldsymbol{e}} = \boldsymbol{A}\boldsymbol{e} + \boldsymbol{B}\left(\boldsymbol{f}(\boldsymbol{x}) + \boldsymbol{G}(\boldsymbol{x})\boldsymbol{u} - \boldsymbol{y}_d^{(n)} + \boldsymbol{d}\right). \tag{3}$$

In the next section, we first describe the variable-structure RBF network that is employed to approximate the unknown function $\boldsymbol{f}(\boldsymbol{x})$ in the adaptive robust controller design.

III. Variable-Structure RBF Network

The employed variable-structure RBF network is an improved version of the self-organizing RBF network used in [14], which, in turn, was adapted from [15]. The major improvement is in the RBF adding and removing operations. Moreover, we introduce a dwelling time T_d, which is a design parameter, into the structure variation of the RBF network to prevent fast switching between different structures.

Our variable-structure RBF network has N different admissible structures, where N is determined by the design parameters discussed later. For each admissible structure illustrated in Fig. 1, the RBF network consists of n input neurons, M_v hidden neurons, where $v \in \{1, \ldots, N\}$ denotes the scalar index, and p output neurons. The k-th output of the RBF network with the v-th admissible structure can be represented as

$$\hat{f}_{k,v}(\boldsymbol{x}) = \sum_{j=1}^{M_v} \omega_{kj,v}\xi_{j,v}(\boldsymbol{x}), \tag{4}$$

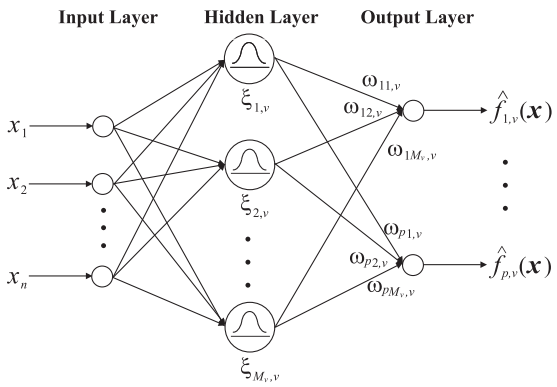

Fig. 1. Self-organizing radial basis function network.

where $\omega_{kj,v}$ is the weight from the j-th hidden neuron to the k-th output neuron and $\xi_{j,v}(\boldsymbol{x})$ is the radial basis function for the j-th hidden neuron. Let $\boldsymbol{W}_v = [\boldsymbol{\omega}_{1,v} \ \cdots \ \boldsymbol{\omega}_{p,v}]$ with $\boldsymbol{\omega}_{i,v} = [\omega_{i1,v} \ \cdots \ \omega_{iM_v,v}]^\top$ and $\boldsymbol{\xi}_v(\boldsymbol{x}) = [\xi_{1,v}(\boldsymbol{x}) \ \cdots \ \xi_{M_v,v}(\boldsymbol{x})]^\top$. Then we have $\hat{\boldsymbol{f}}_v(\boldsymbol{x}) = \boldsymbol{W}_v^\top \boldsymbol{\xi}_v(\boldsymbol{x})$. We employ the raised-cosine RBF proposed in [17] instead of the commonly used Gaussian RBF. The one-dimensional RCRBF is defined as

$$\xi(x) = \begin{cases} \frac{1}{2}\left(1 + \cos\left(\frac{\pi(x-c)}{\delta}\right)\right) & \text{if } |x-c| \leq \delta \\ 0 & \text{if } |x-c| > \delta, \end{cases}$$

where c is the center and δ is the radius. The n-dimensional RCRBF can be represented as the product of n one-dimensional RCRBFs. Although the Gaussian RBF is commonly used for the construction of the radial basis function network, we prefer the raised-cosine RBF to the Gaussian RBF because of the compact support associated with the raised-cosine RBF. As discussed in [15], [17], the compact support of the RCRBF enables fast and efficient training and output evaluation of the RBF network.

In the following subsections, we provide a detailed description of the improved variable-structure RBF network.

A. Center Grid

Recall that the unknown function $\boldsymbol{f}(\boldsymbol{x})$ is approximated over a compact set $\boldsymbol{\Omega}_x \subset \mathbb{R}^n$. Without loss of generality, it is assumed that $\boldsymbol{\Omega}_x$ can be represented as

$$\begin{aligned} \boldsymbol{\Omega}_x &= \{\boldsymbol{x} \in \mathbb{R}^n : \boldsymbol{x}_l \leq \boldsymbol{x} \leq \boldsymbol{x}_u\} \\ &= \{\boldsymbol{x} \in \mathbb{R}^n : x_{li} \leq x_i \leq x_{ui}, \ 1 \leq i \leq n\}, \end{aligned}$$

where the n-dimensional vectors $\boldsymbol{x}_l$ and $\boldsymbol{x}_u$ denote lower and upper bounds of $\boldsymbol{x}$, respectively. To locate the centers of RBFs inside the approximation region $\boldsymbol{\Omega}_x$, we utilize an n-dimensional center grid with layer hierarchy, where each grid node corresponds to the center of one RBF. The grid nodes of the center grid are located at $S_1 \times \cdots \times S_n$, where S_i is the set of locations of the grid nodes in the i-th coordinate and $\times$ denotes the Cartesian product. The center grid is initialized inside the approximation region $\boldsymbol{\Omega}_x$ with $S_i = \{x_{li}, x_{ui}\}$, $i = 1, \ldots, n$. The 2^n grid nodes of the initial grid are referred to as the boundary grid nodes, and they cannot be removed.

In each coordinate, additional grid nodes will be added into and then can be removed from the set S_i as the controlled system evolves in time. However, new grid nodes can only be placed at the potential locations. The potential grid nodes are determined coordinate-wise. In each coordinate, the potential grid nodes of the first layer are the two fixed boundary grid nodes. The second layer has only one potential grid node in the middle of the boundary grid nodes. Then the potential grid nodes of the subsequent layers are in the middle of the adjacent potential grid nodes of all the previous layers.

B. Adding RBFs

As the controlled system evolves in time, the output tracking error $\boldsymbol{e}_y$ is measured. If the Euclidean norm of $\boldsymbol{e}_y$ exceeds a prespecified threshold $e_{\max}$, the network attempts to add new RBFs, that is, add new grid nodes. First, the nearest neighboring grid node in the center grid, denoted $\boldsymbol{c}_{(\text{nearest})}$, to the current input $\boldsymbol{x}$ is located among existing grid nodes. Then the "nearer" neighboring grid node in the center grid denoted $\boldsymbol{c}_{(\text{nearer})}$ is located, where $c_{i(\text{nearer})}$ is determined such that x_i is between $c_{i(\text{nearest})}$ and $c_{i(\text{nearer})}$. Next, the adding operation is performed for each coordinate independently. A new grid node is added into S_i if the following conditions are satisfied:

(1) $\|\boldsymbol{e}_y\| > e_{\max}$;
(2) the elapsed time since the last operation, adding or removing, is greater than T_d;
(3) $\left|x_i - c_{i(\text{nearest})}\right| > \left|c_{i(\text{nearest})} - c_{i(\text{nearer})}\right|/4$;
(4) $\left|x_i - c_{i(\text{nearest})}\right| > d_{i(\text{threshold})}$, where $d_{i(\text{threshold})}$ is a design parameter that specifies the minimum grid distance in the i-th coordinate and thus determines the number of admissible structures denoted by N.

C. Removing RBFs

When the Euclidean norm of the output tracking error $\boldsymbol{e}_y$ is less than or equal to the prespecified threshold $e_{\max}$, the network attempts to remove some of the existing RBFs to prevent network redundancy. The RBF removing operation is also implemented for each coordinate independently. The grid node located at $c_{i(\text{nearest})}$ is removed from S_i if

(1) $\|\boldsymbol{e}_y\| \le e_{\max}$;
(2) the elapsed time since the last operation, adding or removing, is greater than T_d;
(3) $c_{i(\text{nearest})} \notin \{x_{li}, x_{ui}\}$;
(4) the the grid node in the i-th coordinate with its coordinate equal to $c_{i(\text{nearest})}$ is in the higher than or in the same layer as the highest layer of the two neighboring grid nodes in the same coordinate;
(5) $\left|x_i - c_{i(\text{nearest})}\right| < \tau \left|c_{i(\text{nearest})} - c_{i(\text{nearer})}\right|$, for $\tau \in (0,\ 0.5)$.

D. Uniform Grid Transformation

The determination of the radius of the RBF is much easier in a uniform grid than in a nonuniform grid because the RBF is radially symmetric with respect to its center. To simplify the radius determination, the one-to-one mapping $\boldsymbol{z}(\boldsymbol{x}) = [z_1(x_1)\ \cdots\ z_n(x_n)]^\top$, proposed in [17], is used to transform the center grid into a uniform grid. Suppose that the RBF network is now with the v-th admissible structure after the adding or removing operation and there are $M_{i,v}$ distinct elements in S_i ordered as $c_{i(1)} < \cdots < c_{i(M_{i,v})}$, where $c_{i(k)}$ is the k-th element with $c_{i(1)} = x_{li}$ and $c_{i(M_{i,v})} = x_{ui}$. Then the mapping function $z_i(x_i) : [x_{li},\ x_{ui}] \to [1,\ M_{i,v}]$ takes the following form,

$$z_i(x_i) = k + \frac{x_i - c_{i(k)}}{c_{i(k+1)} - c_{i(k)}}, \quad c_{i(k)} \le x_i < c_{i(k+1)} \tag{5}$$

which maps $c_{i(k)}$ into the integer k. Thus, the transformation $\boldsymbol{z}(\boldsymbol{x}) : \boldsymbol{\Omega}_x \to \mathbb{R}^n$ maps the center grid into a grid with unit spacing between adjacent grid nodes such that the radius of the RBF can be easily chosen. For the raised-cosine RBF, the radius in every coordinate is selected to be equal to one unit, that is, the radius will touch but not extend beyond the neighboring grid nodes in the uniform grid. This particular choice of the radius guarantees that for any given input $\boldsymbol{x}$, the number of nonzero raised-cosine RBFs in the uniform grid is at most 2^n.

IV. Adaptive Robust Controller Development

The proposed adaptive robust controller has the form

$$\begin{aligned}\boldsymbol{u} &= \boldsymbol{u}_{a,v} + \boldsymbol{u}_{s,v} \\ &= \boldsymbol{G}_0^{-1}\left(-\hat{\boldsymbol{f}}_v(\boldsymbol{x}) + \boldsymbol{y}_d^{(n)} - \boldsymbol{K}\boldsymbol{e}\right) + \boldsymbol{u}_{s,v},\end{aligned} \tag{6}$$

where $\boldsymbol{G}_0 = g_0\boldsymbol{I}_p$ with $g_0 > 0$, $\hat{\boldsymbol{f}}_v(\boldsymbol{x}) = \boldsymbol{W}_v^\top \boldsymbol{\xi}_v(\boldsymbol{x})$, $\boldsymbol{K} = \text{diag}[\boldsymbol{k}_1\ \ \ldots\ \ \boldsymbol{k}_p]$ is selected such that $\boldsymbol{A}_{mi} = \boldsymbol{A}_i - \boldsymbol{b}_i\boldsymbol{k}_i$ is Hurwitz, and $\boldsymbol{u}_{s,v}$ is the robustifying component to be designed later. Note that the controller architecture varies as the structure of the RBF network changes. A particular controller architecture is referred to as a mode. Because there are N admissible network structures, the proposed controller has N different modes. Let $\boldsymbol{\Omega}_{e_0}$ be a compact set including all possible initial state tracking errors and let $c_{e_0} = \max_{\boldsymbol{e}\in\boldsymbol{\Omega}_{e_0}} \frac{1}{2}\boldsymbol{e}^\top \boldsymbol{P}_m \boldsymbol{e}$, where $\boldsymbol{P}_m = \text{diag}[\boldsymbol{P}_{m1}\ \ \cdots\ \ \boldsymbol{P}_{mp}]$ is the solution to the continuous Lyapunov matrix equation $\boldsymbol{A}_m^\top \boldsymbol{P}_m + \boldsymbol{P}_m \boldsymbol{A}_m = -2\boldsymbol{Q}_m$ for $\boldsymbol{Q}_m = \text{diag}[\boldsymbol{Q}_{m1}\ \cdots\ \boldsymbol{Q}_{mp}]$ with $\boldsymbol{Q}_{mi} = \boldsymbol{Q}_{mi}^\top > 0$. Choose $c_e > c_{e_0}$ and let $\boldsymbol{\Omega}_e = \{\boldsymbol{e} : \frac{1}{2}\boldsymbol{e}^\top \boldsymbol{P}_m \boldsymbol{e} \le c_e\}$. Then we define $\boldsymbol{\Omega}_x = \{\boldsymbol{x} : \boldsymbol{x} = \boldsymbol{e} + \boldsymbol{x}_d, \boldsymbol{e} \in \boldsymbol{\Omega}_e, \boldsymbol{x}_d \in \boldsymbol{\Omega}_{x_d}\}$, over which the unknown function $\boldsymbol{f}(\boldsymbol{x})$ is approximated.

To proceed, recall that $\boldsymbol{W}_v = [\boldsymbol{\omega}_{1,v}\ \cdots\ \boldsymbol{\omega}_{p,v}]$. For the practical implementation, we constrain the weight vectors $\boldsymbol{\omega}_{i,v}$ to reside in the compact sets

$$\boldsymbol{\Omega}_{i,v} = \{\boldsymbol{\omega}_{i,v} : \underline{\omega}_i \le \omega_{ij,v} \le \overline{\omega}_i, 1 \le j \le M_v\},$$

where $\underline{\omega}_i$ and $\overline{\omega}_i$, $i = 1, \ldots, p$, are design parameters. Let $\boldsymbol{W}_v^* = [\boldsymbol{\omega}_{1,v}^*\ \cdots\ \boldsymbol{\omega}_{p,v}^*]$ denote the "optimal" constant weight matrix corresponding to each admissible network structure, which are used only in the analytical analysis and defined as

$$\boldsymbol{W}_v^* = \underset{\boldsymbol{\omega}_{i,v}\in\boldsymbol{\Omega}_{i,v}}{\text{argmin}} \max_{\boldsymbol{x}\in\boldsymbol{\Omega}_x} \left\|\boldsymbol{f}(\boldsymbol{x}) - \boldsymbol{W}_v^\top \boldsymbol{\xi}_v(\boldsymbol{x})\right\|.$$

Let $\boldsymbol{\Phi}_v = \boldsymbol{W}_v - \boldsymbol{W}_v^* = [\boldsymbol{\phi}_{1,v} \ \cdots \ \boldsymbol{\phi}_{p,v}]$ with $\boldsymbol{\phi}_{i,v} = \boldsymbol{\omega}_{i,v} - \boldsymbol{\omega}_{i,v}^*$, and let $c = \sum_{i=1}^p c_i$, where

$$c_i = \max_v \left(\max_{\boldsymbol{\omega}_{i,v}, \boldsymbol{\omega}_{i,v}^* \in \boldsymbol{\Omega}_{i,v}} \frac{1}{2\eta} \boldsymbol{\phi}_{i,v}^\top \boldsymbol{\phi}_{i,v} \right), \tag{7}$$

$\eta > 0$ is a design parameter, and $\max_v(\cdot)$ denotes the maximization taken over all the admissible structures of the RBF networks. It is obvious that c_i decreases as η increases. Let $\boldsymbol{\sigma} = \boldsymbol{B}^\top \boldsymbol{P}_m \boldsymbol{e}$. We employ the following projection based weight matrix adaptation law

$$\dot{\boldsymbol{W}}_v = \mathrm{Proj}\left(\boldsymbol{W}_v, \eta \boldsymbol{\xi}_v(\boldsymbol{x}) \boldsymbol{\sigma}^\top\right), \tag{8}$$

where $\mathrm{Proj}(\boldsymbol{W}_v, \boldsymbol{\Theta}_v)$ denotes $\mathrm{Proj}(\omega_{ij,v}, \theta_{ij,v})$ for $i = 1, \ldots, p$ and $j = 1, \ldots, M_v$ and $\mathrm{Proj}(\omega_{ij,v}, \theta_{ij,v})$ is the discontinuous projection operators used in [14]. For the above projection operator, we have

$$\frac{1}{\eta} \mathrm{trace}\left(\boldsymbol{\Phi}_v^\top \left(\dot{\boldsymbol{W}}_v - \eta \boldsymbol{\xi}_v(\boldsymbol{x}) \boldsymbol{\sigma}^\top \right) \right) \leq 0. \tag{9}$$

Furthermore, the adaptation law (8) guarantees that if $\boldsymbol{\omega}_{i,v}(t_0) \in \boldsymbol{\Omega}_{i,v}$, then $\boldsymbol{\omega}_{i,v}(t) \in \boldsymbol{\Omega}_{i,v}$ for $t \geq t_0$.

Substituting the proposed adaptive robust controller given by (6) into the state tracking error dynamics (3) gives

$$\begin{aligned}
\dot{\boldsymbol{e}} &= \boldsymbol{A}\boldsymbol{e} + \boldsymbol{B}\left(\boldsymbol{f}(\boldsymbol{x}) + \boldsymbol{G}(\boldsymbol{x})(\boldsymbol{u}_{a,v} + \boldsymbol{u}_{s,v}) - \boldsymbol{y}_d^{(n)} + \boldsymbol{d} \right) \\
&= \boldsymbol{A}\boldsymbol{e} + \boldsymbol{B}\left(\hat{\boldsymbol{f}}_v(\boldsymbol{x}) + \boldsymbol{G}_0 \boldsymbol{u}_{a,v} - \boldsymbol{y}_d^{(n)} \right) + \boldsymbol{B}\boldsymbol{G}(\boldsymbol{x})\boldsymbol{u}_{s,v} \\
&\quad + \boldsymbol{B}\left(\boldsymbol{f}(\boldsymbol{x}) - \hat{\boldsymbol{f}}_v(\boldsymbol{x}) + (\boldsymbol{G}(\boldsymbol{x}) - \boldsymbol{G}_0)\boldsymbol{u}_{a,v} + \boldsymbol{d} \right) \\
&= \boldsymbol{A}_m \boldsymbol{e} - \boldsymbol{B}\boldsymbol{\Phi}_v^\top \boldsymbol{\xi}_v(\boldsymbol{x}) + \boldsymbol{B}\boldsymbol{G}(\boldsymbol{x})\boldsymbol{u}_{s,v} \\
&\quad + \boldsymbol{B}\left(\boldsymbol{f}(\boldsymbol{x}) - \boldsymbol{W}_v^{*\top} \boldsymbol{\xi}_v(\boldsymbol{x}) \right) \\
&\quad + \boldsymbol{B}(\boldsymbol{G}(\boldsymbol{x}) - \boldsymbol{G}_0)\boldsymbol{u}_{a,v} + \boldsymbol{B}\boldsymbol{d}.
\end{aligned} \tag{10}$$

As can be seen from (10), the robustifying component $\boldsymbol{u}_{s,v}$ has to counteract the effects of the approximation error as well as the bounded disturbance to force the state tracking error $\boldsymbol{e}$ converge or, at least, be bounded. Let

$$d_f = \max_v \left(\max_{\boldsymbol{x} \in \boldsymbol{\Omega}_x} \left\| \boldsymbol{f}(\boldsymbol{x}) - \boldsymbol{W}_v^{*\top} \boldsymbol{\xi}_v(\boldsymbol{x}) \right\| \right)$$

and $d_g = \max_{\boldsymbol{x} \in \boldsymbol{\Omega}_x} \|\boldsymbol{G}(\boldsymbol{x}) - \boldsymbol{G}_0\|$. We propose a robustifying component $\boldsymbol{u}_{s,v}$ of the form

$$\boldsymbol{u}_{s,v} = \begin{cases} -\frac{k_{s,v}}{\underline{g}} \frac{\boldsymbol{\sigma}}{\|\boldsymbol{\sigma}\|} & \text{if } \|\boldsymbol{\sigma}\| \geq \nu \\ -\frac{k_{s,v}}{\underline{g}} \frac{\boldsymbol{\sigma}}{\nu} & \text{if } \|\boldsymbol{\sigma}\| < \nu, \end{cases} \tag{11}$$

where

$$k_{s,v} = d_f + d_g \|\boldsymbol{u}_{a,v}\| + d_o$$

and $\nu > 0$ is a design parameter.

Remark: Let the increasing sequence $\{t_i\}_{i=0}^\infty$ be a partition of the interval $[t_0, \ \infty)$ such that $v = v_i$ over $[t_i, \ t_{i+1}]$. During the i-th time interval $[t_i, \ t_{i+1}]$, the controller $\boldsymbol{u}$ given by (6) and (11) has a fixed architecture. Thus, as discussed in [21], there exists a unique solution $\boldsymbol{x}_{v_i}(t)$ to (2) starting at $\boldsymbol{x}_{v_i}(t_i)$ over $[t_i, \ t_{i+1}]$. On the other hand, we have imposed the dwelling time requirement on each mode so that $t_{i+1} - t_i \geq T_d$. Therefore, we can piece together the solutions $\boldsymbol{x}_{v_i}(t)$ over $[t_i, \ t_{i+1}]$ to establish the existence of a unique solution $\boldsymbol{x}(t)$ to (2) starting at $\boldsymbol{x}(t_0)$ over $[t_0, \ \infty)$, where $\boldsymbol{x}_{v_0}(t_0) = \boldsymbol{x}(t_0)$ and $\boldsymbol{x}_{v_{i+1}}(t_{i+1}) = \boldsymbol{x}_{v_i}(t_{i+1})$.

Now we consider the following piecewise continuous quadratic Lyapunov function candidate whenever the proposed adaptive robust controller (6) is in the v-th mode,

$$V_v = \frac{1}{2} \boldsymbol{e}^\top \boldsymbol{P}_m \boldsymbol{e} + \frac{1}{2\eta} \mathrm{trace}\left(\boldsymbol{\Phi}_v^\top \boldsymbol{\Phi}_v \right). \tag{12}$$

This Lyapunov function has jump discontinuities when the proposed controller switches between different modes. Evaluating the time derivative of V_v on the solutions to (10) and taking into account (9), we obtain

$$\begin{aligned}
\dot{V}_v &= \boldsymbol{e}^\top \boldsymbol{P}_m \dot{\boldsymbol{e}} + \frac{1}{\eta} \mathrm{trace}\left(\boldsymbol{\Phi}_v^\top \dot{\boldsymbol{\Phi}}_v \right) \\
&= -\boldsymbol{e}^\top \boldsymbol{Q}_m \boldsymbol{e} + \boldsymbol{\sigma}^\top \boldsymbol{G}(\boldsymbol{x}) \boldsymbol{u}_{s,v} + \boldsymbol{\sigma}^\top \boldsymbol{d} \\
&\quad + \boldsymbol{\sigma}^\top \left(\boldsymbol{f}(\boldsymbol{x}) - \boldsymbol{W}_v^{*\top} \boldsymbol{\xi}_v(\boldsymbol{x}) + (\boldsymbol{G}(\boldsymbol{x}) - \boldsymbol{G}_0)\boldsymbol{u}_{a,v} \right) \\
&\quad + \frac{1}{\eta} \mathrm{trace}\left(\boldsymbol{\Phi}_v^\top \dot{\boldsymbol{\Phi}}_v \right) - \boldsymbol{\sigma}^\top \boldsymbol{\Phi}_v^\top \boldsymbol{\xi}_v(\boldsymbol{x}) \\
&\leq -\lambda_{\min}(\boldsymbol{Q}_m) \|\boldsymbol{e}\|^2 + k_{s,v} \|\boldsymbol{\sigma}\| + \boldsymbol{\sigma}^\top \boldsymbol{G}(\boldsymbol{x}) \boldsymbol{u}_{s,v}.
\end{aligned} \tag{13}$$

If $\|\boldsymbol{\sigma}\| > \nu$, we have

$$k_{s,v} \|\boldsymbol{\sigma}\| + \boldsymbol{\sigma}^\top \boldsymbol{G}(\boldsymbol{x}) \boldsymbol{u}_{s,v} \leq k_{s,v} \|\boldsymbol{\sigma}\| - k_{s,v} \|\boldsymbol{\sigma}\| = 0; \tag{14}$$

if $\|\boldsymbol{\sigma}\| \leq \nu$, we have

$$k_{s,v} \|\boldsymbol{\sigma}\| + \boldsymbol{\sigma}^\top \boldsymbol{G}(\boldsymbol{x}) \boldsymbol{u}_{s,v} \leq k_{s,v} \|\boldsymbol{\sigma}\| - k_{s,v} \frac{\|\boldsymbol{\sigma}\|^2}{\nu} \leq \frac{k_{s,v}}{4} \nu. \tag{15}$$

Recall that $k_{s,v} = d_f + d_g \|\boldsymbol{u}_{a,v}\| + d_o$. Let $k_s = d_f + d_g \max_v (\max \|\boldsymbol{u}_{a,v}\|) + d_o$, where the inner maximization is taken over $\boldsymbol{e} \in \boldsymbol{\Omega}_e$, $\boldsymbol{x}_d \in \boldsymbol{\Omega}_{x_d}$, $\boldsymbol{y}_d^{(n)} \in \boldsymbol{\Omega}_{y_d}$ and $\boldsymbol{\omega}_{i,v} \in \boldsymbol{\Omega}_{i,v}$. Combining (14) and (15), we obtain

$$k_{s,v} \|\boldsymbol{\sigma}\| + \boldsymbol{\sigma}^\top \boldsymbol{G}(\boldsymbol{x}) \boldsymbol{u}_{s,v} \leq \frac{k_{s,v}}{4} \nu \leq \frac{k_s}{4} \nu. \tag{16}$$

It follows from (7) that

$$\frac{1}{2\eta} \mathrm{trace}\left(\boldsymbol{\Phi}_v^\top \boldsymbol{\Phi}_v \right) = \sum_{i=1}^p \frac{1}{2\eta} \boldsymbol{\phi}_{i,v}^\top \boldsymbol{\phi}_{i,v} \leq \sum_{i=1}^p c_i = c. \tag{17}$$

Taking into account (16) and (17) in (13) gives

$$\begin{aligned}
\dot{V}_v &\leq -\lambda_{\min}(\boldsymbol{Q}_m) \|\boldsymbol{e}\|^2 + \frac{k_s}{4} \nu \\
&\leq -2\mu_m V_v + 2\mu_m c + \frac{k_s}{4} \nu \\
&\leq -\mu_m V_v - \mu_m (V_v - 2\bar{c}),
\end{aligned} \tag{18}$$

where $\mu_m = \lambda_{\min}(\boldsymbol{Q}_m)/\lambda_{\max}(\boldsymbol{P}_m)$ and $\bar{c} = c + k_s \nu/(8\mu_m)$. Let $t_{0,v}$ and $t_{f,v}$ denote the initial and the final time instant, respectively, of a continuous time period during which the controller is in the v-th mode. It follows from (18) that if $V_v(t) \geq 2\bar{c}$ for $t \in [t_{0,v}, \ t_{f,v}]$, we have $\dot{V}_v(t) \leq -\mu_m V_v(t)$, which implies that

$$V_v(t) \leq \exp(-\mu_m (t - t_{0,v})) V_v(t_{0,v}) \tag{19}$$

for $t \in [t_{0,v}, \ t_{f,v}]$.

Theorem 1: Let t_1, t_2 and t_3 be three consecutive switching time instants so that $v = v_1$ for $t \in [t_1,\ t_2]$ and $v = v_2$ for $t \in [t_2,\ t_3]$. Suppose that $V_v(t) \geq 2\bar{c}$ for $t \in [t_1,\ t_3]$. If the dwelling time T_d of the variable-structure RBF network is selected such that

$$T_d \geq \frac{1}{\mu_m} \ln\left(\frac{3}{2}\right), \tag{20}$$

then $V_{v_2}(t_2) < V_{v_1}(t_1)$ and $V_{v_2}(t_3) < V_{v_1}(t_2)$.

Proof: When the controller switches from the v_1-th to the v_2-th mode, there exists a jump between $V_{v_2}(t_2)$ and $V_{v_1}(t_2)$, which is denoted as

$$\Delta = V_{v_2}(t_2) - V_{v_1}(t_2). \tag{21}$$

We know that $\boldsymbol{e}$ is continuous because $\boldsymbol{x}$ is continuous. Hence, it follows from (12) and (17) that

$$\begin{aligned}\Delta = &\frac{1}{2\eta} \operatorname{trace}\left(\boldsymbol{\Phi}_{v_2}^\top(t_2)\boldsymbol{\Phi}_{v_2}(t_2)\right) \\ &- \frac{1}{2\eta} \operatorname{trace}\left(\boldsymbol{\Phi}_{v_1}^\top(t_2)\boldsymbol{\Phi}_{v_1}(t_2)\right)\end{aligned}$$

and $|\Delta| \leq c$. Because $V_{v_2}(t) \geq 2\bar{c}$ for $t \in [t_2,\ t_3]$, it follows from (19) and (21) that

$$\begin{aligned}V_{v_2}(t_3) &\leq \exp(-\mu_m(t_3 - t_2))V_{v_2}(t_2) \\ &= \exp(-\mu_m(t_3 - t_2))\left(V_{v_1}(t_2) + \Delta\right) \\ &\leq \exp(-\mu_m(t_3 - t_2))\left(V_{v_1}(t_2) + c\right).\end{aligned}$$

Due to the dwelling time requirement on the variable-structure RBF network, we have $t_3 - t_2 \geq T_d$, which implies that $\exp(-\mu_m(t_3 - t_2)) \leq \exp(-\mu_m T_d)$. Thus, we have $V_{v_2}(t_3) \leq \exp(-\mu_m T_d)\left(V_{v_1}(t_2) + c\right)$. In order to have $V_{v_2}(t_3) < V_{v_1}(t_2)$, it is sufficient to have

$$\exp(-\mu_m T_d)\left(V_{v_1}(t_2) + c\right) < V_{v_1}(t_2). \tag{22}$$

Solving (22) for T_d, we obtain

$$T_d > \frac{1}{\mu_m} \ln\left(\frac{V_{v_1}(t_2) + c}{V_{v_1}(t_2)}\right).$$

It is easy to verify that the right-hand side of the above inequality is a decreasing function of $V_{v_1}(t_2)$ when $V_{v_1}(t_2) \geq 2\bar{c}$. Recall that $\bar{c} > c$. It follows that

$$\ln\left(\frac{V_{v_1}(t_2) + c}{V_{v_1}(t_2)}\right) \leq \ln\left(\frac{2\bar{c} + c}{2\bar{c}}\right) < \ln\left(\frac{3}{2}\right).$$

Therefore, if we choose T_d to satisfy the condition (20), then (22) is satisfied, which implies that $V_{v_2}(t_3) < V_{v_1}(t_2)$.

On the other hand, because $V_{v_1}(t) \geq 2\bar{c}$ for $t \in [t_1,\ t_2]$, it follows from (19) that $V_{v_1}(t_2) \leq \exp(-\mu_m(t_2 - t_1))V_{v_1}(t_1)$, which implies that

$$V_{v_1}(t_1) \geq \exp(\mu_m(t_2 - t_1))V_{v_1}(t_2) \geq \exp(\mu_m T_d)V_{v_1}(t_2),$$

because $t_2 - t_1 \geq T_d$. Note that, for the condition given by (20), we have $V_{v_1}(t_2) > \exp(-\mu_m T_d)\left(V_{v_1}(t_2) + c\right)$. Then it follows that

$$\begin{aligned}V_{v_1}(t_1) &\geq \exp(\mu_m T_d)V_{v_1}(t_2) \\ &> V_{v_1}(t_2) + c \geq V_{v_1}(t_2) + \Delta = V_{v_2}(t_2).\end{aligned}$$

Hence, if the dwelling time T_d satisfies the condition (20), then $V_{v_2}(t_2) < V_{v_1}(t_1)$ and $V_{v_2}(t_3) < V_{v_1}(t_2)$. The proof of the theorem is complete. ■

Theorem 2: Consider the system (2) driven by the proposed adaptive robust controller (6) and (11) with the adaptation laws (8). Suppose that T_d satisfies (20). If $c_e \geq \max\{c_{e_0} + c,\ 2\bar{c} + c\}$, then $\boldsymbol{e}(t) \in \boldsymbol{\Omega}_e$ and $\boldsymbol{x}(t) \in \boldsymbol{\Omega}_x$ for $t \geq t_0$. Moreover, there exists a finite time $T_1 \geq t_0$ such that $\frac{1}{2}\boldsymbol{e}^\top(t)\boldsymbol{P}_m\boldsymbol{e}(t) \leq 2\bar{c} + c$ for $t \geq T_1$. If, in addition, there exists a finite time $T_s \geq t_0$ such that $v = v_s$ for $t \geq T_s$, then there exists a finite time $T_2 \geq T_s$ such that $\frac{1}{2}\boldsymbol{e}^\top(t)\boldsymbol{P}_m\boldsymbol{e}(t) \leq 2\bar{c}$ for $t \geq T_2$.

Proof: If T_d satisfies (20), it follows from Theorem 1 that $V_v(t)$ will visit the interval $[0,\ 2\bar{c}]$ infinitely often. That is, for any $T \geq t_0$, there exists a time $t \geq T$ such that $V_v(t) \leq 2\bar{c}$. Let $T_1 \geq t_0$ be the first time such that $V_v(T_1) \leq 2\bar{c}$. The trajectory of $V_v(t)$ starting at $t = T_1$ will stay inside the interval $[0,\ 2\bar{c}]$ until it jumps outside when the controller switches the mode. However, the jump of $V_v(t)$ between different modes satisfies that $|\Delta| \leq c$. Hence, we have $V_v(t) \leq 2\bar{c} + c$ for $t \geq T_1$. On the other hand, we know that $V_v(t_0) \leq c_{e_0} + c$. Therefore, if $c_e \geq \max\{c_{e_0} + c,\ 2\bar{c} + c\}$, then $V_v(t) \leq c_e$ for $t \geq t_0$. Because $\frac{1}{2}\boldsymbol{e}^\top(t)\boldsymbol{P}_m\boldsymbol{e}(t) \leq V_v(t)$, we have $\frac{1}{2}\boldsymbol{e}^\top(t)\boldsymbol{P}_m\boldsymbol{e}(t) \leq c_e$, which implies that $\boldsymbol{e}(t) \in \boldsymbol{\Omega}_e$ and $\boldsymbol{x}(t) \in \boldsymbol{\Omega}_x$, for $t \geq t_0$. Moreover, we have $\frac{1}{2}\boldsymbol{e}^\top(t)\boldsymbol{P}_m\boldsymbol{e}(t) \leq 2\bar{c} + c$ for $t \geq T_1$.

If, in addition, we have $v = v_s$ for $t \geq T_s$, then it follows from (18) that $\dot{V}_{v_s} \leq -\mu_m V_{v_s} - \mu_m(V_{v_s} - 2\bar{c})$ for $t \geq T_s$. Thus, there exists a finite time $T_2 \geq T_s$ such that $V_{v_s} \leq 2\bar{c}$, which implies that $\frac{1}{2}\boldsymbol{e}^\top(t)\boldsymbol{P}_m\boldsymbol{e}(t) \leq 2\bar{c}$, for $t \geq T_2$. The proof of the theorem is complete. ■

V. Example

We illustrate the effectiveness of the proposed variable-structure RCRBF network based adaptive robust controller with a planar articulated two-link manipulator, whose model is given in [22, p. 394]. Recall that q_1 and q_2 denote the angular positions of joint 1 and 2, respectively, and τ_1 and τ_2 denote the applied torques. We assume that there exist input disturbances η_1 and η_2 associated with the applied torques τ_1 and τ_2, respectively. The dynamics of this two-link rigid robot are described by

$$\begin{aligned}&\begin{bmatrix} H_{11} & H_{12} \\ H_{21} & H_{22} \end{bmatrix}\begin{bmatrix} \ddot{q}_1 \\ \ddot{q}_2 \end{bmatrix} \\ &\quad + \begin{bmatrix} -h\dot{q}_2 & -h\left(\dot{q}_1 + \dot{q}_2\right) \\ h\dot{q}_1 & 0 \end{bmatrix}\begin{bmatrix} \dot{q}_1 \\ \dot{q}_2 \end{bmatrix} = \begin{bmatrix} \tau_1 + \eta_1 \\ \tau_2 + \eta_2 \end{bmatrix},\end{aligned}$$

where $H_{11} = a_1 + 2a_3\cos(q_2) + 2a_4\sin(q_2)$, $H_{12} = H_{21} = a_2 + a_3\cos(q_2) + a_4\sin(q_2)$, $H_{22} = a_2$ and $h = a_3\sin(q_2) - a_4\cos(q_2)$ with $a_1 = I_1 + m_1 l_{c1}^2 + I_e + m_e l_{ce}^2 + m_e l_1^2$, $a_2 = I_e + m_e l_{ce}^2$, $a_3 = m_e l_1 l_{ce}\cos(\delta_e)$ and $a_4 = m_e l_1 l_{ce}\sin(\delta_e)$. The same plant model was also used in [9], [11] to test the proposed controllers there but without input disturbances, that is, $\boldsymbol{\eta} = \boldsymbol{0}$. In our simulation, we use the same numerical values as in [9], [11], [22, p. 396], that is,

$$\begin{aligned}&m_1 = 1.0 \quad m_e = 2.0 \quad I_1 = 0.12 \quad I_e = 0.25 \\ &l_{c1} = 0.5 \quad l_{ce} = 0.6 \quad l_1 = 1 \qquad \delta_e = \pi/6.\end{aligned}$$

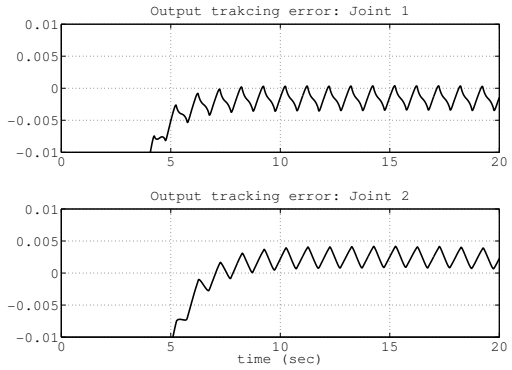

Fig. 2. Tracking errors e_1 and e_2.

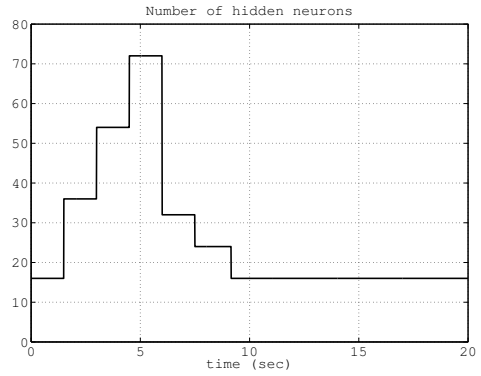

Fig. 3. Variation of the number of grid nodes.

We select the input disturbances η_1 and η_2 to be the band-limited white noise signals. The manipulator is initially at rest, that is, $q_1 = q_2 = 0$ and $\dot{q}_1 = \dot{q}_2 = 0$.

We consider the same reference signals as in [11], which are defined as

$$q_{d1}(t) = \frac{\pi}{6}\cos(2\pi t) \quad \text{and} \quad q_{d2}(t) = \frac{\pi}{4}\cos(2\pi t).$$

Thus, we choose the grid boundaries for q_1, $\dot{q}_1$, q_2 and $\dot{q}_2$ to be $[-1.0\ 1.0]$, $[-4.0\ 4.0]$, $[-1.0\ 1.0]$ and $[-5.5\ 5.5]$, respectively. For the controller, we choose $\boldsymbol{k}_1 = [1\ 2]$, $\boldsymbol{k}_2 = [4\ 4]$, $\boldsymbol{Q}_1 = \boldsymbol{Q}_2 = 0.5\boldsymbol{I}_2$, $d_f = d_g = d_o = 5$, $\nu = 0.025$, $\underline{g} = 0.1$ and $\boldsymbol{G}_0 = 2\boldsymbol{I}_2$. The rest of the design parameters of the variable-structure RCRBF network are selected as $e_{\max} = 0.005$, $\boldsymbol{d}_{\text{threshold}} = [0.2\ 0.3\ 0.2\ 0.3]$, $\underline{\omega}_1 = \underline{\omega}_2 = -25$, $\overline{\omega}_1 = \overline{\omega}_2 = 25$, $\eta = 500$ and $T_d = 1.5$. In Fig. 2 and Fig. 3, we show the performance of the proposed adaptive robust controller.

VI. Conclusions

A novel adaptive robust controller has been proposed for the output tracking control of a class of MIMO uncertain systems, where a variable-structure RBF network is used to approximate unknown system dynamics. The RBF network can grow or shrink on-line dynamically according to the tracking performance. The raised-cosine RBF was employed in order to guarantee the overall computational efficiency. To account for the effects of the structure variation of the RBF network in the stability analysis of the closed-loop system, the piecewise continuous Lyapunov function for switched and hybrid systems was used. Simulation results confirm the effectiveness of the proposed adaptive robust controller.

References

[1] I. Kanellakopoulos, P. V. Kokotovic, and R. Marino, "An extended direct scheme for robust adaptive nonlinear control," *Automatica*, vol. 27, no. 2, pp. 247–255, 1991.

[2] A. Kojic and A. M. Annaswamy, "Adaptive control of nonlinearly parameterized systems with a triangular structure," *Automatica*, vol. 38, no. 1, pp. 115–123, 2002.

[3] M. Krstic and P. V. Kokotovic, "Adaptive nonlineaer design with controller-identifier separation and swapping," *IEEE Trans. Autom. Control*, vol. 40, no. 3, pp. 426–460, Mar. 1995.

[4] E. B. Kosmatopoulos and P. A. Ioannou, "Robust switching adaptive control of multi-input nonlinear systems," *IEEE Trans. Autom. Control*, vol. 47, no. 4, pp. 610–624, Apr. 2002.

[5] R. M. Sanner and J. J. E. Slotine, "Gaussian networks for direct adaptive control," *IEEE Trans. Neural Netw.*, vol. 3, no. 6, pp. 837–863, Nov. 1992.

[6] A. Yesildirek and F. L. Lewis, "Feedback linearization using neural networks," *Automatica*, vol. 31, no. 11, pp. 1659–1664, 1995.

[7] S. Seshagiri and H. K. Khalil, "Output feedback control of nonlinear systems using RBF neural networks," *IEEE Trans. Neural Netw.*, vol. 11, no. 1, pp. 69–79, Jan. 2000.

[8] Y. Lee, S. Hui, E. Zivi, and S. H. Żak, "Variable neural adaptive robust controllers for uncertain systems," *Int. J. Adapt. Control Signal Process.*, vol. 22, no. 8, pp. 721–738, 2008.

[9] C.-C. Liu and F.-C. Chen, "Adaptive control of non-linear continuous-time systems using neural networks—general relative degree and MIMO cases," *Int. J. Contr.*, vol. 58, no. 2, pp. 317–335, 1993.

[10] Y.-C. Chang, "An adaptive H^∞ tracking control for a class of nonlinear multiple-input-multiple-output (MIMO) systems," *IEEE Trans. Autom. Control*, vol. 46, no. 9, pp. 1432–1437, Sep. 2001.

[11] H. Xu and P. A. Ioannou, "Robust adaptive control for a class of MIMO nonlinear systems with guaranteed error bounds," *IEEE Trans. Autom. Control*, vol. 48, no. 5, pp. 728–742, May 2003.

[12] C. P. Bechlioulis and G. A. Rovithakis, "Robust adaptive control of feedback linearizable MIMO nonlinear systems with prescribed performance," *IEEE Trans. Autom. Control*, vol. 53, no. 9, pp. 2090–2099, Oct. 2008.

[13] G. P. Liu, V. Kadirkamanathan, and S. A. Billings, "Variable neural networks for adaptive control of nonlinear systems," *IEEE Trans. Syst., Man, Cybern. B*, vol. 39, no. 1, pp. 34–43, Feb. 1999.

[14] J. Lian, Y. Lee, and S. H. Żak, "Variable neural direct adaptive robust control of uncertain systems," *IEEE Trans. Autom. Control*, vol. 53, no. 11, pp. 2658–2664, Dec. 2008.

[15] J. Lian, Y. Lee, S. D. Sudhoff, and S. H. Żak, "Self-organizing radial basis function network for real-time approximation of continuous-time dynamical systems," *IEEE Trans. Neural Netw.*, vol. 19, no. 3, pp. 460–474, Mar. 2008.

[16] J. P. Hespanha and A. S. Morse, "Stability of switched systems with average dwell-time," in *Proc. 38th Conference on Decision and Control*, Phoenix, Arizona, Dec. 1999, pp. 2655–2660.

[17] R. J. Schilling, J. J. Carroll, and A. F. Al-Ajlouni, "Approximation of nonlinear systems with radial basis function neural network," *IEEE Trans. Neural Netw.*, vol. 12, no. 1, pp. 1–15, Jan. 2001.

[18] M. S. Branicky, "Multiple Lyapunov functions and other analysis tools for switched and hybrid systems," *IEEE Trans. Autom. Control*, vol. 43, no. 4, pp. 475–482, 1998.

[19] M. Johansson and A. Rantzer, "Computation of piecewise quadratic Lyapunov functions for hybrid systems," *IEEE Trans. Autom. Control*, vol. 43, no. 4, pp. 555–559, Apr. 1998.

[20] J. Lian, J. Hu, and S. H. Żak, "Adaptive robust control: A switched system approach," revised and re-submitted to *IEEE Trans. Autom. Control*, 2009.

[21] M. M. Polycarpou and P. A. Ioannou, "On the existence and uniqueness of solutions in adaptive control systems," *IEEE Trans. Autom. Control*, vol. 38, no. 3, pp. 474–479, Mar. 1993.

[22] J.-J. Slotine and W. Li, *Applied Nonlinear Control*. Englewood Cliffs, NJ: Prentice Hall, 1991.